

# Dependence of Epitaxial $\text{Ba}(\text{Fe}_{1-x}\text{Co}_x)_2\text{As}_2$ Thin Films Properties on $\text{SrTiO}_3$ Template Thickness

S. Lee, J. Jiang, J. D. Weiss, C. W. Bark, C. Tarantini, M. D. Biegalski, A. Polyanskii, Y. Zhang, C. T. Nelson, X. Q. Pan, E. E. Hellstrom, D. C. Larbalestier, and C. B. Eom

**Abstract**—In our previous report, we demonstrated the growth of high-quality epitaxial Co-doped  $\text{Ba}(\text{Fe}_{1-x}\text{Co}_x)_2\text{As}_2$  (Ba-122) thin films using single crystalline  $\text{SrTiO}_3$  (STO) templates on  $(\text{La}, \text{Sr})(\text{Al}, \text{Ta})\text{O}_3$  (LSAT) substrates with pulsed laser deposition (PLD). Here, we report the dependence of the structural and superconducting properties of Ba-122 thin films on STO templates that were 2–150 unit cell (u.c.) thick. We obtained genuine epitaxial thin films with high crystalline quality and excellent superconducting properties for templates above a critical thickness, which was 50 u.c. for our growth condition. Although the quality of Ba-122 is excellent above the critical thickness, the best crystalline quality and superconducting properties were obtained on 100 u.c.-thick STO templates. The best-quality Ba-122 thin films show an on-set transition temperature ( $T_{c, \text{on-set}}$ ) as high as 22.8 K, a transition width ( $\Delta T_c$ ) as narrow as 1.3 K, and critical current density ( $J_c$ ) as high as 3 MA/cm<sup>2</sup>.

**Index Terms**—Iron pnictides, pulsed laser deposition, templates, thin films.

## I. INTRODUCTION

HERE is great interest in studying the intrinsic properties and technological applications of the newly discovered iron pnictide superconductors [1]–[4]. Growth of epitaxial thin films with excellent superconducting properties has been difficult, particularly the F-doped, rare-earth 1111 phase that has the highest  $T_c$  [5]–[8]. Because F is volatile at the growth temperatures it has been very difficult to control the stoichiometry of F-doped 1111 thin films. In contrast,  $\text{Ba}(\text{Fe}_{1-x}\text{Co}_x)_2\text{As}_2$  (Ba-122) is better suited for growing thin film using Co, which

has a low vapor pressure, as the dopant. Epitaxial growth of Ba-122 thin films was reported by us and other groups [9]–[18]. Ba-122,  $\text{SrTiO}_3$  (STO), and  $\text{BaTiO}_3$  (BTO) all contain divalent alkaline-earth (AE) elements, whereas other perovskite oxides such as  $(\text{La}, \text{Sr})(\text{Al}, \text{Ta})\text{O}_3$  (LSAT) or  $\text{LaAlO}_3$  (LAO) contain trivalent (or higher) elements. Building on the idea of having common cation valence in the substrate and Ba-122, we grew high-quality Co-doped Ba-122 epitaxial thin films on (001)-oriented STO bicrystal substrates [17]. However, the STO substrates became electrically conducting during deposition of the Co-doped Ba-122 thin film at 750°C in the high vacuum ( $\sim 10^{-6}$  Torr), owing to formation of oxygen vacancies in the STO [19]. This provides a parallel, current-sharing path between the Ba-122 and STO that compromises the normal-state property studies. By employing either an STO or BTO template on various perovskite substrates, we demonstrated the growth of genuine epitaxial Ba-122 thin films on non-conducting substrate with excellent crystalline and superconducting properties [18]. We found that having an STO or BTO template is critical for growing epitaxial Ba-122 with our growth conditions. In this paper, we show the dependence of the properties of Ba-122 thin films on the STO template thickness. We found that a minimum template thickness is needed to suppress the formation of in-plane misoriented Ba-122 grains. We also found there is an optimum template thickness to obtain the Ba-122 structural and superconducting properties.

## II. EXPERIMENTAL

Epitaxial STO thin film templates were grown on (001) LSAT substrates at 750°C in 8 mTorr of oxygen by pulse laser deposition (PLD). High-pressure reflection high-energy electron diffraction (RHEED) was used for digital control [20] and *in situ* monitoring of the growth. The thicknesses of the STO templates we studied were 2, 20, 50, 100, and 150 unit cells (u.c.). We measured the surface roughness and crystalline quality of STO templates as a function of the STO thickness with atomic force microscopy (AFM) and x-ray diffraction (XRD), respectively. For all the templates, the root mean square (RMS) values measured with AFM are about 0.2 nm, which means the surface roughness is the same regardless of the template thickness. (The AFM image is not shown here.) All the STO templates are perfect single crystalline with extremely sharp rocking curves. The full width at half maximum (FWHM) values of the rocking curve for the STO 002 reflections are  $\sim 0.016^\circ$ . Note: We were not able to determine the crystalline quality of 2 u.c. STO because it was too thin to be measured with XRD. Fig. 1 shows the 002 rocking curve scans of 100 and 150-u.c.-thick STO templates (20 u.c. and 50 u.c. STO are not shown here, but the shape

Manuscript received September 01, 2010; accepted October 19, 2010. Date of publication February 28, 2011; date of current version May 27, 2011. This work was supported in part by the US Department of Energy under Grant DE-FG02-06ER46327 (C.B.E.), by the State of Florida under NSF Cooperative Agreement DMR-0084173, and by AFOSR under Grant FA9550-06-1-0474 (E.E.H. and D.C.L.), and the US Department of Energy under Grant DE-FG02-07ER46416 (X.Q.P.).

S. Lee, C. W. Bark, and C. B. Eom are with the Department of Materials Science and Engineering, University of Wisconsin-Madison, Madison, WI 53706, USA (e-mail: slee83@wisc.edu; bark@wisc.edu; eom@engr.wisc.edu).

J. Jiang, J. D. Weiss, C. Tarantini, A. Polyanskii, E. E. Hellstrom, and D. C. Larbalestier are with the Applied Superconductivity Center, National High Magnetic Field Laboratory, Florida State University, Tallahassee, FL 32310, USA (e-mail: jjiang@asc.magnet.fsu.edu; weiss@asc.magnet.fsu.edu; tarantini@asc.magnet.fsu.edu; polyanskii@asc.magnet.fsu.edu; hellstrom@asc.magnet.fsu.edu; larbalestier@asc.magnet.fsu.edu).

M. D. Biegalski is with the Center for Nanophase Materials Sciences, Oak Ridge National Laboratory, Oak Ridge, TN 37830, USA (e-mail: biegal-skim@ornl.gov).

Y. Zhang, C. T. Nelson, and X. Q. Pan are with the Department of Materials Science and Engineering, The University of Michigan, Ann Arbor, MI 48109, USA (e-mail: yizh@umich.edu; ctnelson@umich.edu; panx@umich.edu).

Digital Object Identifier 10.1109/TASC.2011.2107722

TABLE I  
CRYSTALLINE QUALITY AND SUPERCONDUCTING PROPERTIES OF BA-122 THIN FILMS

	Ba-122/STO templates/LSAT				
	2 u.c.	20 u.c.	50 u.c.	100 u.c.	150 u.c.
Template thickness	2 u.c.	20 u.c.	50 u.c.	<b>100 u.c.</b>	150 u.c.
FWHM $\Delta\omega$ of Ba-122 004 reflection	1.45	0.96	0.84	<b>0.55</b>	0.84
FWHM $\Delta\phi$ of off-axis Ba-122 112 reflection	2.71	1.65	0.98	<b>0.8</b>	0.97
Extra peaks in $\phi$ scan	Yes	Yes	<b>No</b>	<b>No</b>	<b>No</b>
$T_{c, \text{onset}}$ (K)	18.9	20.5	20.7	<b>22.8</b>	21.6
$\Delta T$ (K)	n/a	4.2	1.2	<b>1.3</b>	1.6
$J_c$ (4.2K, Self field) ( $\text{A}/\text{cm}^2$ )	$2.3 \times 10^4$	$5.6 \times 10^5$	$1.7 \times 10^6$	<b><math>2.9 \times 10^6</math></b>	$2.2 \times 10^6$

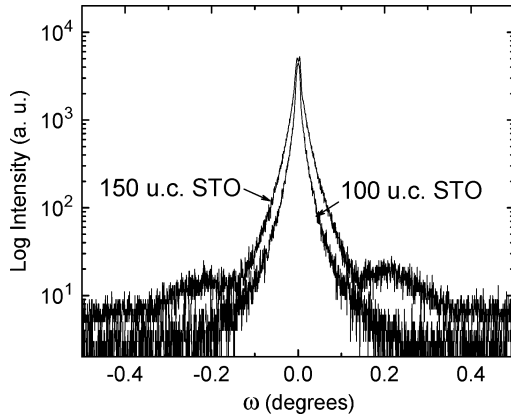


Fig. 1. XRD rocking curves of STO 002 reflection for 100 and 150 u.c. thick STO templates on (001) LSAT substrate.

is the same as 100 u.c. STO). Although the FWHM is comparable for both films, there are shoulders (satellite peaks) on both sides of the main peak for 150 u.c. STO, due to dislocations and partial strain relaxation. This means that the STO templates are fully coherent to the LSAT substrates up to 100 u.c. STO. On top of these STO templates, we grew 350-nm-thick Ba-122 thin films with PLD in vacuum at  $750^\circ\text{C}$ . The detailed growth conditions were reported elsewhere [18]. The Ba-122 targets were prepared by solid-state reaction and had a nominal composition of  $\text{Ba}/\text{Fe}/\text{Co}/\text{As} = 1 : 1 : 84 : 0 : 16 : 2 : 2$ . Based on wavelength dispersive X-ray spectroscopy, the typical composition of our Ba-122 thin film was  $\text{Ba} : \text{Fe} : \text{Co} : \text{As} : \text{O} = 1 : 1.7 : 0.13 : 1.7 : 0.3$ . The structural and superconducting properties of Ba-122 thin films are listed in Table I.

### III. RESULTS AND DISCUSSION

The crystalline quality and the epitaxial arrangement of Ba-122 thin films on different template thicknesses were determined with four-circle XRD. Fig. 2(a) shows  $\theta - 2\theta$  scans of the Ba-122 grown on the 100 u.c. STO/LSAT. The XRD pattern shows that the film 00 $l$  reflections dominate, which indicates the  $c$ -axis growth is normal to the STO template and the LSAT substrate. Ba-122 films on different STO thicknesses have the same out-of-plane texture (not shown here) although the intensity of the Ba-122 00 $l$  peaks is weaker in Ba-122 grown

on thinner STO templates. An extra peak at  $2\theta \approx 65^\circ$  is identified as 002 reflection of Fe; it has low intensity, being less than 5% of the Ba-122 004 reflection. The in-plane texture of Ba-122 was determined with azimuthal  $\phi$  scans of the off-axis 112 peak, as shown in Fig. 2(b). The films grown on the 2 and 20 u.c. STO templates on LSAT exhibit extra peaks at intermediate  $\phi$  angles in addition to the major peaks at every  $90^\circ$ . This indicates that the Ba-122 films contain misoriented grains in the plane with 001 tilt high-angle grain boundaries [18]. In contrast, the Ba-122 films on 50, 100 and 150 u.c. thick STO on LSAT show only strong peaks at every  $90^\circ$ , which indicates that these films have a genuine epitaxial arrangement in the plane. We determined the out-of-plane and in-plane mosaic spreads and crystalline quality of the films by performing rocking curve and azimuthal  $\phi$ -scans, respectively.

Fig. 2(c) shows the FWHM values of the Ba-122 004 rocking curve ( $\Delta\omega$ ) and  $\Delta\phi$  as a function of the STO template thickness. Both the FWHM  $\Delta\omega$  and  $\Delta\phi$  values rapidly decreased from 2 u.c. to 50 u.c. reaching the minimum at the STO thickness of 100 u.c. This trend is consistent with the high in-plane texture and absence of misoriented Ba-122 grains for STO thicknesses above 50 u.c. as shown in Fig. 2(b). We can make three conclusions from the XRD data. First, a minimum template thickness of 50 u.c. STO is needed to obtain genuine epitaxy. Second, the optimum template thickness is 100 u.c. Finally, the high crystalline quality of Ba-122 is maintained above the minimum template thickness (about 50 u.c.) but is slightly compromised above the optimum thickness (about 100 u.c.). This might be due to the compromised STO template quality due to surface defects, dislocations, and partial strain relaxation that form above 100 u.c. as shown in Fig. 1.

The superconducting transition temperature ( $T_c$ ) and transition width ( $\Delta T_c$ ) were determined by a resistivity measurement. The resistivity of the films with a size of about  $2 \text{ mm} \times 4 \text{ mm}$  was measured in a Quantum Design PPMS by a four-point probe method with the current flow along the sample length. As shown in Fig. 3(a), the films grown on 20, 50, 100, and 150 u.c. STO show a residual resistivity ratio of  $\sim 1.9$ , which is similar to Ba-122 bulk single crystal [21]. However, as shown in Fig. 3(b), the film on 20 u.c. STO shows a double transition, which indicates the film contains inhomogeneous superconducting phases.

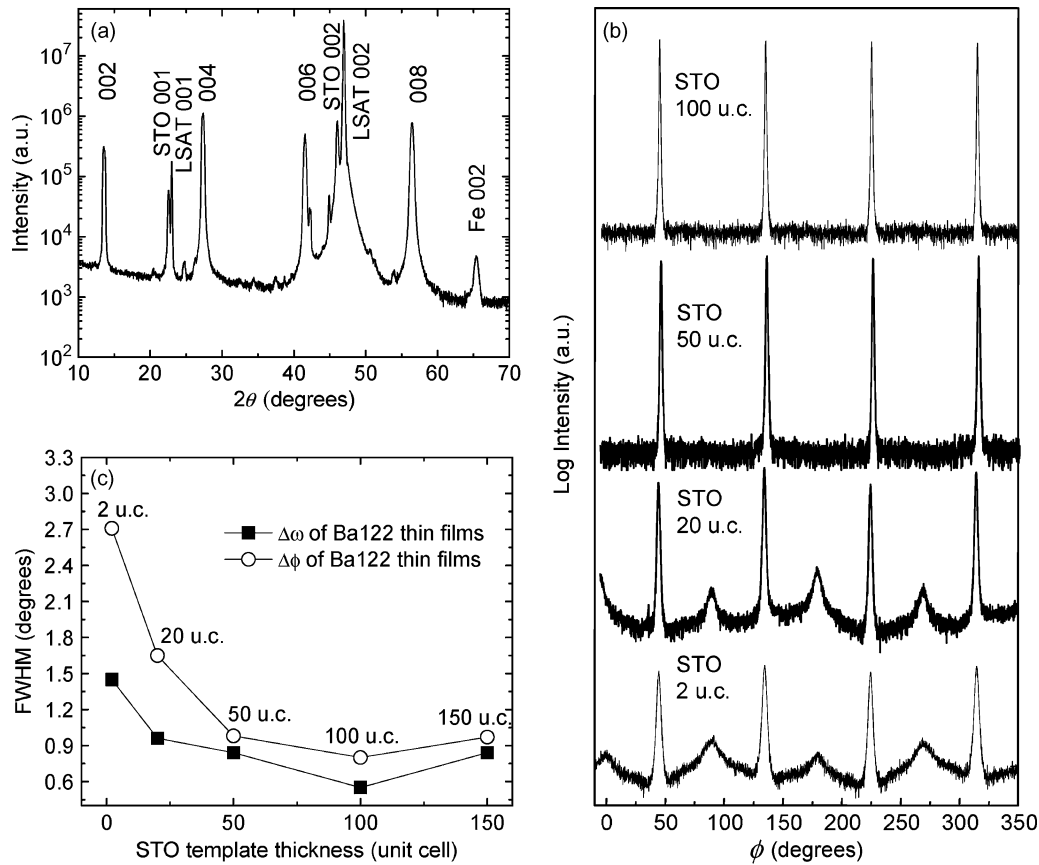


Fig. 2. XRD analysis of Ba-122 films (a) Out-of-plane  $\theta - 2\theta$  scan of Ba-122/100 u.c. STO/LSAT. All non-identified peaks are reflections of identified peaks resulting from  $\text{CuK}\beta$  and  $\text{CuK}\alpha + \beta$ . (b) azimuthal  $\phi$  scan of the off-axis 112 reflections for Ba-122/2, 20, 50, and 100 u.c. STO/LSAT (c) FWHM values of 002 rocking curves ( $\Delta\omega$ ) and the off-axis 112 reflections ( $\Delta\phi$ ) for all Ba-122 films as a function of the STO template thickness.

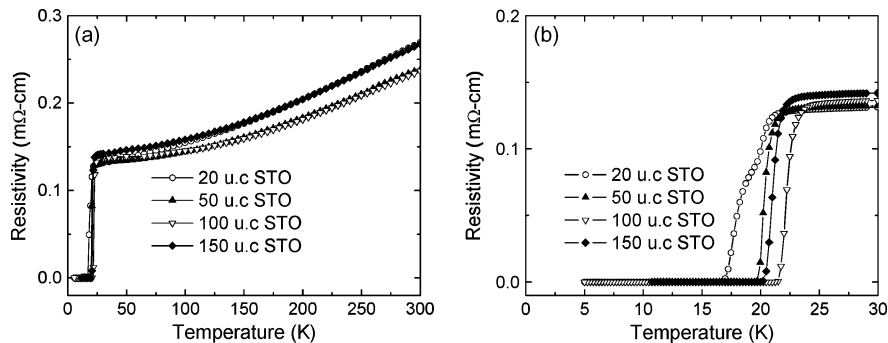


Fig. 3. Resistivity as a function of temperature for the Ba-122 thin films grown on 20, 50, 100, and 150 u.c. STO templates.

Films with on STO with thickness  $\geq 50$  u.c. show narrow transition width. As listed in Table I and Fig. 3(b), both the on-set  $T_c(T_{c, on-set})$  and  $\Delta T_c$  are improved from 2 u.c. STO to 100 u.c. STO and degraded ongoing to 150 u.c. STO. This is consistent with the trend in the crystalline properties of the film. In particular, the film grown on the optimum template thickness (100 u.c. STO) shows the highest  $T_{c, on-set}$  of 22.8 K with a  $\Delta T_c$  of 1.3 K, which is almost the narrowest.

Fig. 4 shows the zero-field-cooled magnetization  $T_c$  transitions of Ba-122 thin films grown on 20, 50, 100, and 150 u.c. STO templates on LSAT. All films have a similar, strong diamagnetic signal except the film grown on the 20 u.c. STO template. The film on the 20 u.c. STO shows granularity associated

with the inability of the screening currents to develop across the high-angle grain boundaries in this film. In contrast, the film grown on the 100 u.c. STO/LSAT shows a strong signal and the highest magnetization  $T_c$ , which is consistent with resistivity  $T_c$  measurement.

Fig. 5 shows the critical current density ( $J_c$ ) as a function of the applied magnetic field for Ba-122 films grown on 20, 50, 100, and 150 u.c. STO templates measured with an Oxford vibrating sample magnetometer (VSM) up to 14 T. Magnetization as a function of temperature was measured by a Quantum Design SQUID magnetometer with a field of 2 mT perpendicular to the film surface. The magnetization loop of the films, which were about 2 mm  $\times$  4 mm, was measured in the VSM at 4.2K

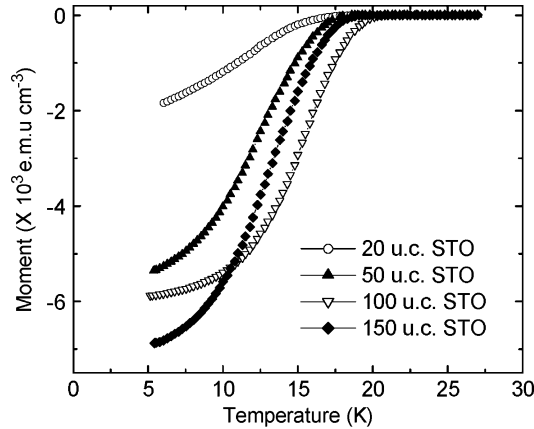


Fig. 4. Magnetic moment as a function of temperature for Ba-122 grown on 20, 50, 100, and 150 u.c. STO templates by warming after zero-field-cooling. A field of 2mT was applied perpendicular to the plane of the films after cooling to 4.2 K.

with the applied field perpendicular to the film surface. Magneto-optical imaging was used to examine the uniformity of current flow in the films to validate the use of the Bean model for converting the magnetic moment measured in the VSM to  $J_c$  assuming current circulation across the whole sample without granular effects. For a thin film,  $J_c = 15 \Delta m / (V \cdot r)$ , where  $\Delta m$  is the width of the hysteresis loop in emu,  $V$  the film volume in  $\text{cm}^3$ , and  $r$  the radius corresponding to the total area of the sample size, and was calculated from  $\pi r^2 = a \times b$  ( $a$  and  $b$  are the film width and length in cm, respectively). Here all films show higher  $J_c$  than that of bulk single crystal ( $0.4 \text{ MA/cm}^2$  at 4.2 K; [22]). Furthermore, the  $J_c$  of the epitaxial films on the 100 and 150 u.c. STO shows a weak field dependence, indicative of little or no suppression of the  $J_c$  by strong magnetic fields. Those films had  $J_c$  up to about  $0.4 \text{ MA/cm}^2$  even at 13 T. According to transmission electron microscopy (TEM) analysis, this is due to the second-phase self-assembled nano-pillars in the Ba-122 matrix, which could act as a very effective pinning center as shown in our previous report [23]. However, the films on the 50, 100, and 150 u.c. STO template have much higher  $J_c$ , by a factor of 5, than the film on the 20 u.c. STO. We believe this is due to the superior epitaxial arrangement in Ba-122 on thicker STO templates (above 50 u.c.) as confirmed by XRD analysis, while the films on the 2 and 20 u.c. STO template have high-angle grain boundaries within the in-plane structure. According to our previous report [17],  $J_c$  in [001] Ba-122 on STO bicrystal substrates with  $\theta = 6^\circ - 24^\circ$  misorientation angles shows significant suppression. It makes sense that randomly-oriented, high-angle tilt grain boundaries in Ba-122 films on the thinner STO templates (2 and 20 u.c.) would effectively block the supercurrent, as suggested by several recent pnictide film reports [5]–[11].

Compared with Ba-122 thin films grown on bare LSAT, even Ba-122 films grown on the 2 u.c. STO template on LSAT are significantly improved in terms of crystalline quality. This indicates that the template itself is critical for growing Ba-122 thin films. However, as shown so far, an STO template that is  $\sim 50$  u.c. thick is needed to grow genuine epitaxial Ba-122 thin

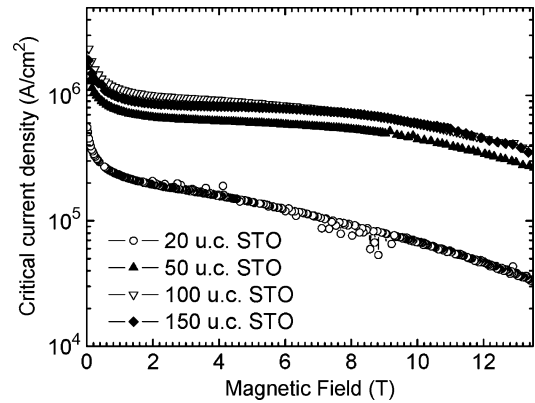


Fig. 5. Critical current density as a function of applied magnetic field at 4.2K for Ba-122 grown on 20, 50, 100, 150 u.c. STO templates.

films without any misoriented grains. We believe the  $45^\circ$  rotated grains in the Ba-122 films grown on thinner STO templates are caused by the solid state reactions during the growth of the Ba-122 film in a 3D island growth mode. When the Ba-122 phase grows on a thinner STO template, the chemical reaction between the LSAT substrate (through atomic diffusion across a few nanometer thick STO template) and Ba-122 will occur. Due to the 3D island growth nature, this reaction occurs randomly on the surface of the STO template and results in the formation of small islands of impurity phase (the product of chemical reaction between LSAT and Ba-122). We believe that these islands of the impurity phase are in favor of the growth of  $45^\circ$  rotated Ba-122 grains, while the remaining STO surface ensures the epitaxial growth of normally oriented Ba-122 film. The extent of such chemical reaction decreases with the increase of the STO template layer, thus, the volume fraction of  $45^\circ$  oriented grains in the Ba-122 films decreases as the STO template thickness as shown in Fig. 2, in consistent with TEM observations.

Transmission electron microscopy (TEM) also showed some localized disorder of the atomic arrangement at the interface between Ba-122 and the STO template [18] This disorder might be evidence of interdiffusion between the Ba-122 and STO template occurring under our growth condition ( $\sim 10^{-6}$  Torr,  $750^\circ\text{C}$ ). We believe a thicker STO template provides an effective diffusion barrier between Ba-122 and the LSAT substrate so that the epitaxial growth of Ba-122 is maintained throughout the growth of Ba-122 films. In our growth condition, 50 u.c. is the minimum thickness for an effective diffusion barrier. Beyond the optimum template thickness of 100 u.c., the quality of Ba-122 is slightly reduced. We believe this is due to various defects generated by a partial strain relaxation of STO templates.

#### IV. SUMMARY

We studied the influence of single crystalline STO template thickness on the properties of epitaxial Ba-122 thin films over the thickness range of 2–150 u.c. STO on (001) LSAT substrates. We obtained genuine epitaxial Ba-122 thin films on STO templates for STO thicknesses  $\geq 50$  u.c. with our Ba-122 growth conditions. We believe that a minimum STO thickness is needed to effectively block interdiffusion between

Ba-122 and the LSAT substrate during the growth of Ba-122 thin films. The Ba-122 films with the best crystalline quality and superconducting properties were grown on the 100 u.c. STO templates, which is the thickest STO template that is still completely coherent with the LSAT substrate. Beyond this optimum STO thickness (100 u.c.), the crystalline properties of Ba-122 are slightly degraded owing to compromised STO crystalline quality due to surface defects, threading dislocation, and strain relaxation of the STO template.

## REFERENCES

- [1] Y. Kamihara, T. Watanabe, M. Hirano, and H. Hosono, "Iron-based layered superconductor  $\text{La}[\text{O}_{1-x}\text{F}_x]\text{FeAs}$  ( $x = 0.05\text{--}0.12$ ) with  $T_C = 26$  K," *J. Am. Chem. Soc.*, vol. 130, pp. 3296–3297, 2008.
- [2] X. H. Chen, T. Wu, G. Wu, R. H. Liu, H. Chen, and D. F. Fang, "Superconductivity at 43 K in  $\text{SmFeAsO}_{1-x}\text{F}_x$ ," *Nature*, vol. 453, p. 761, 2008.
- [3] C. Wang, L. Li, S. Chi, Z. Zhu, Z. Ren, Y. Li, Y. Wang, X. Lin, Y. Luo, S. Jiang, X. Xu, G. Cao, and Z. Xu, "Thorium-doping-induced superconductivity up to 56 K in  $\text{Gd}_{1-x}\text{Th}_x\text{FeAsO}$ ," *Europhys. Lett.*, vol. 83, p. 67006, 2008.
- [4] M. Rotter, M. Tegel, and D. Johrendt, "Superconductivity at 38 K in the iron arsenide  $\text{Ba}_{1-x}\text{K}_x\text{Fe}_2\text{As}_2$ ," *Phys. Rev. Lett.*, vol. 101, p. 107006, 2008.
- [5] H. Hiramatsu, T. Katase, T. Kamiya, M. Hirano, and H. Hosono, "Heteroepitaxial growth and optoelectronic properties of layered iron oxyarsenide,  $\text{LaFeAsO}$ ," *Appl. Phys. Lett.*, vol. 93, p. 162504, 2008.
- [6] S. Haindl, M. Kidszun, A. Kauffmann, K. Nenkov, N. Kozlova, J. Freudenberger, T. Thersleff, J. Hänisch, J. Werner, E. Reich, L. Schultz, and B. Holzapfel, "High upper critical fields and evidence of weak link behaviour in superconducting  $\text{LaFeAsO}_{1-x}\text{F}_x$  thin films," *Phys. Rev. Lett.*, vol. 104, p. 077001, 2010.
- [7] M. Kidszun, S. Haindl, E. Reich, J. Hänisch, K. Iida, L. Schultz, and B. Holzapfel, "Epitaxial  $\text{LaFeAsO}_{1-x}\text{F}_x$  thin films grown by pulsed laser deposition," *Supercond. Sci. Tech.*, vol. 23, p. 022002, 2010.
- [8] M. Kidszun, S. Haindl, T. Thersleff, J. Werner, M. Langer, J. Hänisch, K. Iida, E. Reich, L. Schultz, and B. Holzapfel, "Fabrication of superconducting oxypnictide thin films," *Europhys. Lett.*, vol. 90, p. 57005, 2010.
- [9] H. Hiramatsu, T. Katase, T. Kamiya, M. Hirano, and H. Hosono, "Superconductivity in epitaxial films of Co-doped  $\text{SrFe}_2\text{As}_2$  with bilayered FeAs structures and their magnetic anisotropy," *Applied Physics Express*, vol. 1, p. 101702, 2008.
- [10] T. Katase, H. Hiramatsu, H. Yanagi, T. Kamiya, M. Hirano, and H. Hosono, "Atomically-flat, chemically-stable, superconducting epitaxial thin film of iron-based superconductor, cobalt-doped  $\text{BaFe}_2\text{As}_2$ ," *Solid State Commun.*, vol. 149, pp. 2121–2124, 2009.
- [11] E.-M. Choi, S.-G. Jung, N. H. Lee, Y.-S. Kwon, W. N. Kang, D. H. Kim, M.-H. Jung, S.-I. Lee, and L. Sun, "In situ fabrication of cobalt-doped  $\text{SrFe}_2\text{As}_2$  thin films by using pulsed laser deposition with excimer laser," *Appl. Phys. Lett.*, vol. 95, p. 062507, 2009.
- [12] K. Iida, J. Hänisch, R. Hühne, F. Kurth, M. Kidszun, S. Haindl, J. Werner, L. Schultz, and B. Holzapfel, "Strong  $T_C$  dependence for strained epitaxial  $\text{Ba}(\text{Fe}_{1-x}\text{Co}_x)_2\text{As}_2$  thin films," *Appl. Phys. Lett.*, vol. 95, p. 192051, 2009.
- [13] K. Iida, J. Hänisch, T. Thersleff, F. Kurth, M. Kidszun, S. Haindl, R. Hühne, L. Schultz, and B. Holzapfel, "Scaling behaviour of the critical current in clean epitaxial  $\text{Ba}(\text{Fe}_{1-x}\text{Co}_x)_2\text{As}_2$  thin films," *Phys. Rev. B*, vol. 81, p. 100507, 2010.
- [14] T. Thersleff, K. Iida, S. Haindl, M. Kidszun, D. Pohl, A. Hartmann, F. Kurth, J. Hänisch, R. Hühne, B. Rellinghaus, L. Schultz, and B. Holzapfel, "Coherent interfacial bonding on the FeAs tetrahedron in  $\text{Fe}/\text{Ba}(\text{Fe}_{1-x}\text{Co}_x)_2\text{As}_2$  bilayers," *Appl. Phys. Lett.*, vol. 97, p. 3457432, 2010.
- [15] T. Katase, Y. Ishimaru, A. Tsukamoto, H. Hiramatsu, T. Kamiya, K. Tanabe, and H. Hosono, "Josephson junction in cobalt-doped  $\text{BaFe}_2\text{As}_2$  epitaxial thin films on  $(\text{La}, \text{Sr})(\text{Al}, \text{Ta})\text{O}_3$  bicrystal substrates," *Appl. Phys. Lett.*, vol. 96, p. 3371814, 2010.
- [16] T. Katase, H. Hiramatsu, T. Kamiya, and H. Hosono, "High critical current density 4 MA/cm<sup>2</sup> in Codoped  $\text{BaFe}_2\text{As}_2$  epitaxial films grown on  $(\text{La}, \text{Sr})(\text{Al}, \text{Ta})\text{O}_3$  substrat without buffer layers," *Applied Physics Express*, vol. 3, p. 063101, 2010.
- [17] S. Lee, J. Jiang, J. D. Weiss, C. M. Folkman, C. W. Bark, C. Tarantini, A. Xu, D. Abraimov, A. Polyanskii, C. T. Nelson, H. W. Jang, A. Yamamoto, F. Kametani, X. Q. Pan, A. Gurevich, C. B. Eom, and D. C. Larbalestier, "Weaklin behavior of grain boundaries in superconductor  $\text{Ba}(\text{Fe}_{1-x}\text{Co}_x)_2\text{As}_2$  bicrystal," *Appl. Phys. Lett.*, vol. 95, p. 212505, 2009.
- [18] S. Lee, J. Jiang, Y. Zhang, C. W. Bark, J. D. Weiss, C. Tarantini, C. T. Nelson, H. W. Jang, C. M. Folkman, S. H. Baek, A. Polyanskii, D. Abraimov, A. Yamamoto, J. W. Park, X. Q. Pan, E. E. Hellstrom, D. C. Larbalestier, and C. B. Eom, "Template engineering of Co-doped  $\text{BaFe}_2\text{As}_2$  single-crystal thin films," *Nature Materials*, vol. 9, pp. 397–402, 2010.
- [19] G. Herranz, M. Basletić, M. Bibes, C. Carrétéro, E. Tafra, E. Jacquet, K. Bouzehouane, C. Deranlot, A. Hamzić, J.-M. Broto, A. Barthélémy, and A. Fert, "High Mobility in  $\text{LaAlO}_3/\text{SrTiO}_3$  Heterostructures: Origin, Dimensionality, and Perspectives," *Phys. Rev. Lett.*, vol. 98, p. 216803, 2007.
- [20] G. J. H. M. Rijnders, G. Koster, D. H. A. Blank, and H. Rogalla, "In situ monitoring during pulsed laser deposition of complex oxides using reflection high energy electron diffraction under high oxygen pressure," *Appl. Phys. Lett.*, vol. 70, p. 1888, 1997.
- [21] A. S. Sefat, R. Jin, M. A. McGuire, B. C. Sales, D. J. Singh, and D. Mandrus, "Superconductivity at 22 K in Co-doped  $\text{BaFe}_2\text{As}_2$  crystals," *Phys. Rev. Lett.*, vol. 101, p. 117004, 2010.
- [22] A. Yamamoto, J. Jaroszynski, C. Tarantini, L. Balicas, J. Jiang, A. Gurevich, D. C. Larbalestier, R. Jin, A. S. Sefat, M. A. McGuire, B. C. Sales, D. K. Christen, and D. Mandrus, "Small anisotropy, weak thermal fluctuations, and high field superconductivity in Co-doped iron pnictide  $\text{Ba}(\text{Fe}_{1-x}\text{Co}_x)_2\text{As}_2$ ," *Appl. Phys. Lett.*, vol. 94, p. 062511, 2009.
- [23] C. Tarantini, S. Lee, Y. Zhang, J. Jiang, C. W. Bark, J. D. Weiss, A. Polyanskii, C. T. Nelson, H. W. Jang, C. M. Folkman, S. H. Baek, X. Q. Pan, A. Gurevich, E. E. Hellstrom, C. B. Eom, and D. C. Larbalestier, "Strong vortex pinning in Co-doped  $\text{BaFe}_2\text{As}_2$  single crystal thin films," *Appl. Phys. Lett.*, vol. 96, p. 3383237, 2010.